PNAS RESEARCH ARTICLE | DEVELOPMENTAL BIOLOGY OPEN ACCESS

Lysosomes are required for early dorsal signaling in the *Xenopus* embryo

Nydia Tejeda-Muñoz[a] and Edward M. De Robertis[a,1]

Contributed by Edward M. De Robertis; received January 18, 2022; accepted March 23, 2022; reviewed by Makoto Asashima and Anming Meng

Lysosomes are the digestive center of the cell and play important roles in human diseases, including cancer. Previous work has suggested that late endosomes, also known as multivesicular bodies (MVBs), and lysosomes are essential for canonical Wnt pathway signaling. Sequestration of Glycogen Synthase 3 (GSK3) and of β-catenin destruction complex components in MVBs is required for sustained canonical Wnt signaling. Little is known about the role of lysosomes during early development. In the *Xenopus* egg, a Wnt-like cytoplasmic determinant signal initiates formation of the body axis following a cortical rotation triggered by sperm entry. Here we report that cathepsin D was activated in lysosomes specifically on the dorsal marginal zone of the embryo at the 64-cell stage, long before zygotic transcription starts. Expansion of the MVB compartment with low-dose hydroxychloroquine (HCQ) greatly potentiated the dorsalizing effects of the Wnt agonist lithium chloride (LiCl) in embryos, and this effect required macropinocytosis. Formation of the dorsal axis required lysosomes, as indicated by brief treatments with the vacuolar ATPase (V-ATPase) inhibitors Bafilomycin A1 or Concanamycin A at the 32-cell stage. Inhibiting the MVB-forming machinery with a dominant-negative point mutation in Vacuolar Protein Sorting 4 (Vps4-EQ) interfered with the endogenous dorsal axis. The Wnt-like activity of the dorsal cytoplasmic determinant Huluwa (Hwa), and that of microinjected xWnt8 messenger RNA, also required lysosome acidification and the MVB-forming machinery. We conclude that lysosome function is required for early dorsal axis development in *Xenopus*. The results highlight the intertwining between membrane trafficking, lysosomes, and vertebrate axis formation.

lysosomes | cytoplasmic determinant | *Xenopus laevis* | Wnt signaling | Hwa

Significance

The dorsal axis of the vertebrate *Xenopus* embryo is established by an early Wnt signal generated by a rotation of the cortex of the egg toward the opposite side of the sperm entry point. In this study, we report that lysosomal cathepsin D becomes activated on the dorsal marginal zone of the embryo already at the 64-cell stage, and that this asymmetry is enhanced by increasing Wnt signaling levels. We present experiments showing that lysosome acidification, macropinocytosis, and multivesicular body formation are required for the endogenous dorsal signal provided maternally in the egg. The results indicate that the cell biology of lysosomes plays an essential role in vertebrate development.

In *Xenopus* development, formation of the Spemann organizer and subsequent axial development is controlled by a dorsal Wnt-like signal resulting from a microtubule-driven rotation of egg cortical cytoplasm toward the opposite side of the sperm entry point (1, 2). This signal is known to involve the displacement of cytoplasmic membrane vesicles located on the vegetal pole that contain Dishevelled (Dvl) (3, 4). Recently, it has been proposed that the zebrafish maternal determinant is a novel transmembrane protein called Huluwa (Hwa), which causes degradation of the Wnt pathway component Axin1 in dorsal blastomeres (5). While all transcriptional effects of Wnt signaling are mediated by the stabilization of β-catenin (6, 7), recent work has revealed that membrane trafficking is also essential for Wnt signaling (8–10). The inhibition of glycogen synthase 3 kinase (GSK3) after binding to the Wnt receptors Lrp6 and Frizzled triggers macropinocytosis, an actin-driven cell drinking process (11, 12) by which extracellular proteins are engulfed and trafficked to lysosomes for degradation (12, 13). The increased membrane trafficking leads to the formation of multivesicular bodies (MVBs) that sequester GSK3 and Axin1, resulting in a marked increase in lysosomal acidification and activation of lysosomal enzymes (13).

Here we report that the active form of the lysosomal enzyme cathepsin D localizes to dorsal cells at the 64-cell stage in *Xenopus* embryos, and that this activation is greatly increased by microinjection of *xWnt8* messenger RNA (mRNA) or the GSK3 inhibitor lithium chloride (LiCl). Expanding the MBV late endosomal compartment by microinjecting low-dose hydroxychloroquine (HCQ) potentiated dorsal signaling by LiCl. This effect was blocked by microinjection of 5-*N*-ethyl-*N*-isopropylamiloride (EIPA), a macropinocytosis inhibitor. In the intact embryo, Spemann organizer formation and central nervous system (CNS) induction were inhibited by a short treatment with the vacuolar ATPase (V-ATPase) inhibitor Bafilomycin A1 (Baf) or by interfering with MVB formation. Signaling by microinjected *xHwa* mRNA was blocked by Baf treatment at the 32-cell stage, coinjection with EIPA, or inhibitors of the ESCRT (Endosomal Sorting Complexes Required for Transport) machinery. We conclude that lysosomes play an essential role in the initiation of axis formation by the dorsal cytoplasmic determinant.

Author affiliations: [a]Department of Biological Chemistry, David Geffen School of Medicine, University of California, Los Angeles, CA 90095-1662

Author contributions: N.T.-M. and E.M.D.R. designed research, performed research, analyzed data, and wrote the paper.

Reviewers: M.A., Teikyo Daigaku; and A.M., Tsinghua University.

The authors declare no competing interest.

[1]To whom correspondence may be addressed. Email: ederobertis@mednet.ucla.edu.

This article contains supporting information online at http://www.pnas.org/lookup/suppl/doi:10.1073/pnas.2201008119/-/DCSupplemental.

Published April 21, 2022.

Results

Activated Lysosomes in the Dorsal Side at the 64-Cell Stage. Cortical rotation in *Xenopus* results in a less pigmented dorsal crescent that marks the future dorsal side during early development (Fig. 1 *A* and *A*') (14). Embryos at the 64-cell stage were fixed, bisected, and stained with Sir-Lysosome, a very useful reagent that specifically labels active lysosomes by binding to the activated, cleaved form of lysosomal cathepsin D via a pepstatin A peptide (13, 15). An enrichment in active lysosomes was observed in the dorsal marginal cells of uninjected control embryos (Fig. 1 *B* and *B*'). This asymmetry was strongly enhanced by microinjection of *xWnt8* mRNA (16) or LiCl (17) (Fig. 1 *C* and *D*'). The increased activation of dorsal lysosomal cathepsin D could also be observed at the blastula stage (Fig. 1 *E*–*G*''). In addition, LiCl microinjection caused a striking stabilization of the V-ATPase subunit V0a3 (18), particularly on the dorsal side of the embryo (*SI Appendix*, Fig. S1 *A* and *B*). The stabilization of V-ATPase, the enzyme that acidifies the endolysosomal pathway and controls membrane trafficking, is consistent with previous observations that GSK3 inhibition increases macropinocytosis and subsequent lysosomal acidification (13). The results indicate that lysosomes are activated in the dorsal side of the embryo at early cleavage stages, long before zygotic transcription is activated.

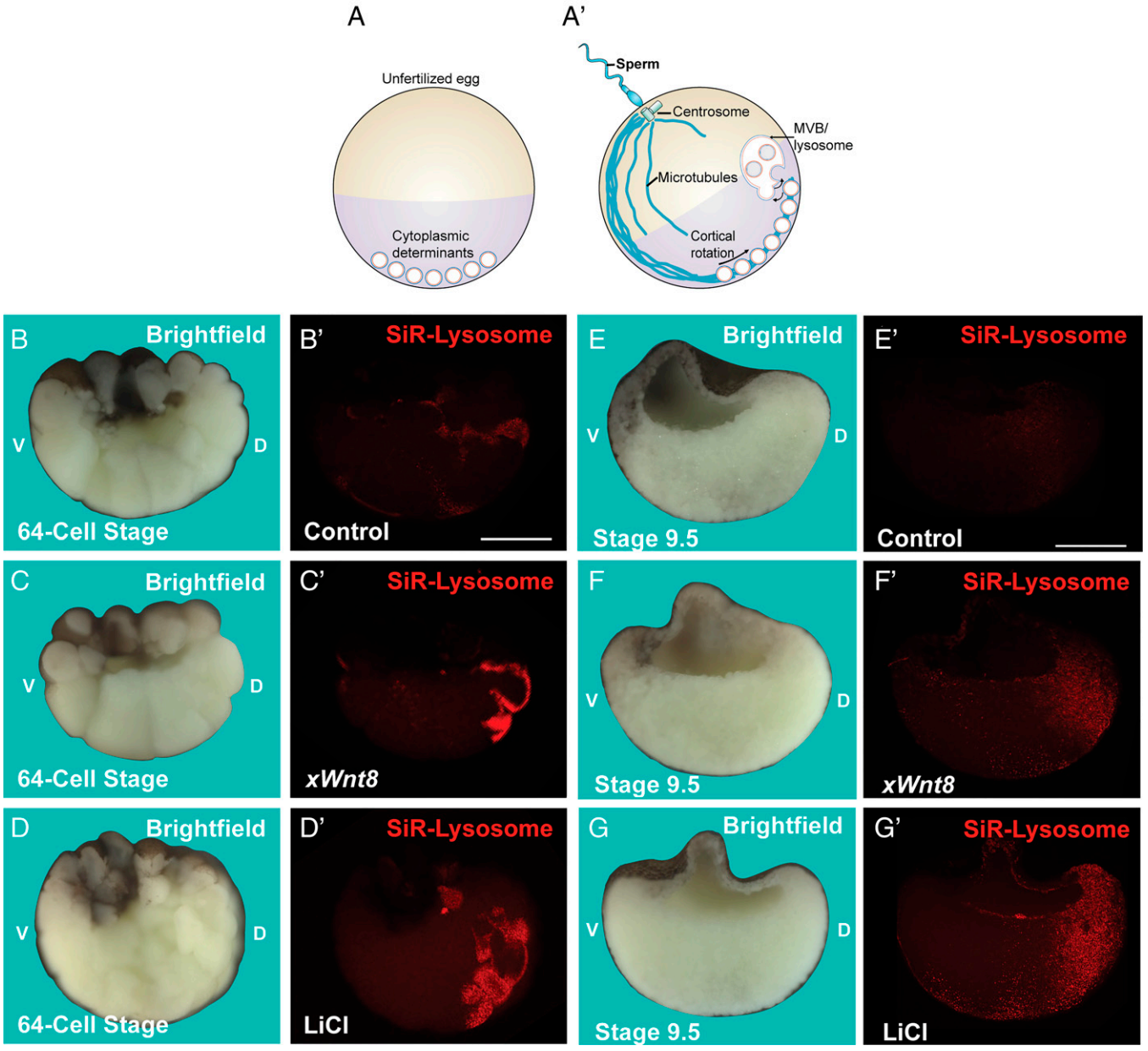

Fig. 1. Lysosomes are activated on the dorsal side at the 64-cell stage embryos, and this asymmetry is increased by *xWnt8* mRNA or LiCl microinjection. (*A*) The unfertilized egg contains cytoplasmic determinants indicated by membrane-bounded organelles that contain Dvl. (*A*') Sperm entry introduces the centrosome which nucleates microtubules that drive cortical rotation of cytoplasmic determinants. The hypothesis tested here is that MVBs and lysosomes are activated by the maternal Wnt-like signal. (*B* and *B*') SiR-lysosome fluorophore stains activated cathepsin D in dorsal cells at the 64-cell stage. (*C*'–*D*') Microinjection of 2 pg of *xWnt8* mRNA or 4 nL of 300 mM LiCl into the vegetal pole at four cells greatly increases active lysosomes. (*E*–*G*') The increase in lysosomal active cathepsin D induced by Wnt and LiCl was also observed at the blastula stage. D, dorsal; V, ventral. Numbers of embryos analyzed were as follows: B = 31, 100%; C = 29, 93.2%; D = 32, about 90% with dorsal signal, five independent experiments; E = 27, 100%; F = 31; 92%; G = 25, 94%. (Scale bars, 500 μm.) See also *SI Appendix*, Fig. S1.

Low-Dose HCQ Increases Wnt and LiCl Signaling. We have shown that low doses of the lysosomotropic antimalarial drug chloroquine (CQ) can increase Wnt signaling twofold to threefold by expanding the MVB compartment and facilitating the sequestration of GSK3 and Axin1 in MVBs (19). We now report that its derivative, HCQ, is more effective than CQ, increasing Wnt3a-induced β-catenin activated reporter (BAR) expression (20) up to 34 times in cultured mammalian cells (Fig. 2*A*). In the absence of Wnt, HCQ had no stimulatory effect (Fig. 2*A*). At high concentrations, HCQ, like CQ, had the opposite effect, inhibiting Wnt by alkalinizing the endosomal compartment (*SI Appendix*, Fig. S2 *A–G*). In the presence of Wnt, HCQ enhanced nuclear β-catenin in SW480 cells reconstituted with wild-type APC, only at low doses, while causing stabilization of CD63, a marker of MVB intraluminal vesicles (21), at both low and high doses (*SI Appendix*, Fig. S2 *H–L*'). In colorectal cancer SW480 cells, which have constitutive Wnt signaling due to mutation of the tumor suppressor APC, endogenous GSK3 and Axin1 antigens were present in intracellular puncta that partially colocalized with the MVB marker CD63 (*SI Appendix*, Fig. S3 *A* and *D*). When lysosomal alkalinization was inhibited with high-dose HCQ or Baf, GSK3 and Axin1 levels were decreased and were no longer detected in MVBs (*SI Appendix*, Fig. S3 *A–F*).

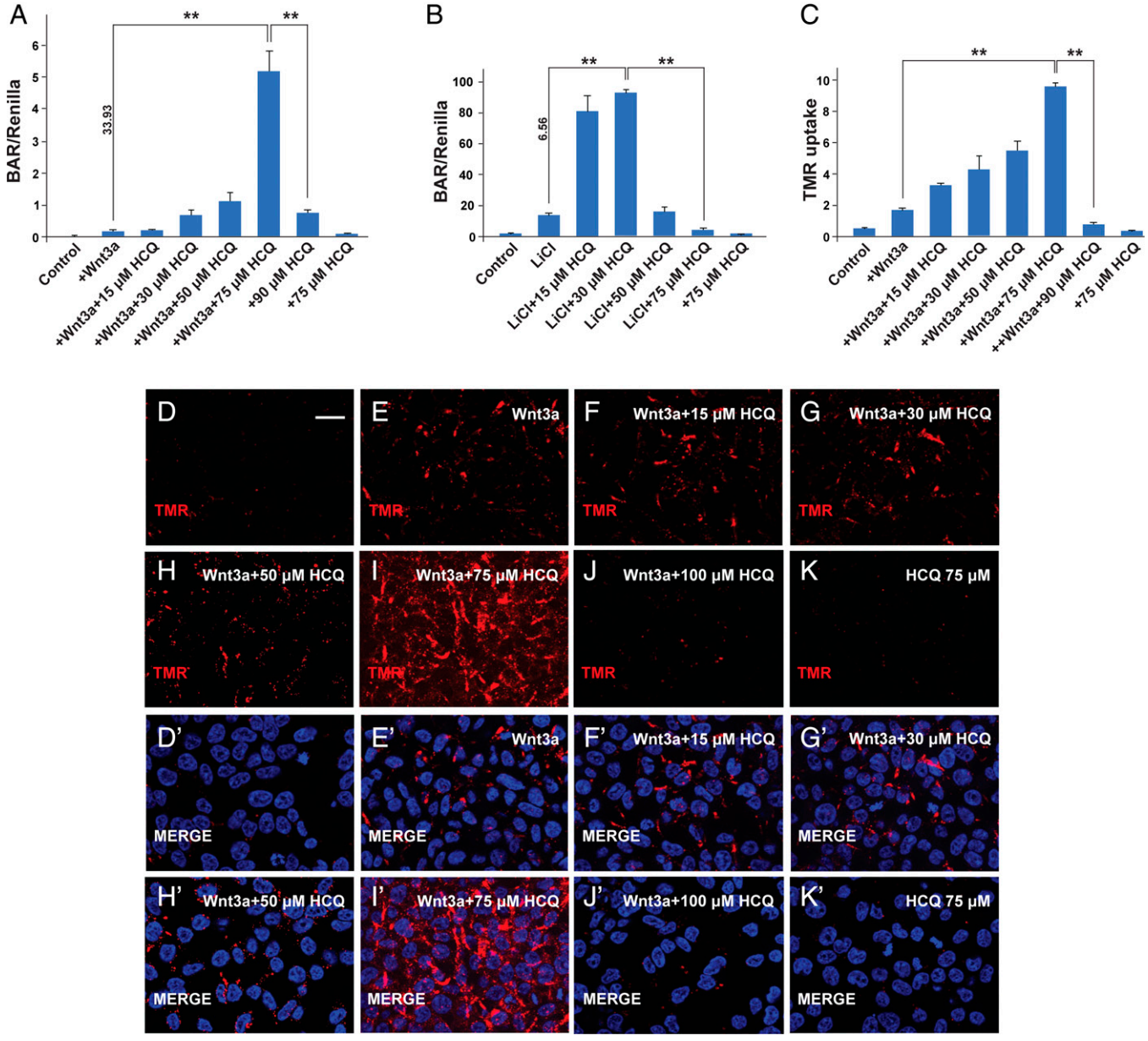

Fig. 2. Wnt3a, LiCl transcriptional activity, and macropinocytosis are potentiated by low-dose HCQ. All assays were performed in HEK293-BR cells that contain stably integrated BAR and Renilla reporter genes. (*A*) Wnt3a treatment for 18 h was strongly potentiated by 75 μM HCQ and inhibited by higher concentrations. (*B*) HCQ increased LiCl-induced β-catenin signaling but at lower concentrations. (*C*) Macropinocytosis of TMR-dextran 70 kDa was stimulated by low doses of HCQ and inhibited at high levels. Note that, in all cases, HCQ was without effect in the absence of Wnt or LiCl treatment. Experiments represent biological triplicates. Error bars denote SEM ($n \geq 3$) (**$P < 0.01$). (*D* and *D'*) HEK-293T cells have very low levels of macropinocytosis after 1 h of incubation with a macropinocytosis marker TMR-dextran 70 kDa. (*E* and *E'*) Addition of Wnt3a (100 ng/mL) increases macropinocytosis. (*F–I"*) The addition of HCQ potentiates Wnt-stimulated macropinocytosis, particularly at 75 μM HCQ. (*G* and *G"*) At higher concentrations (100 μM), HCQ inhibits macropinocytosis. (*K* and *K"*) HCQ alone (75 μM) has no effect on macropinocytosis. Wnt3a induced micropinocytosis, and this is greatly potentiated by low-dose HCQ and inhibited by high dose HCQ, while HCQ alone has no effect on macropinocytosis The results of a similar experiment to that shown here were quantified by spectrophotometry in *C*. (Scale bars, 10 μm.) See also *SI Appendix*, Figs. S2 and S3.

The transcriptional β-catenin signal triggered by the GSK3 inhibitor LiCl was enhanced by low-dose HCQ, although the optimal concentration level was different from that of Wnt3a (Fig. 2*B*). Wnt3a triggers macropinocytosis of tetramethylrhodamine (TMR)-dextran 70 kDa (12) which has a hydrated diameter over 200 nm and is the gold standard for measuring macropinocytosis. Low-dose HCQ potentiated Wnt-induced macropinocytosis, while high doses inhibited it (Fig. 2 *C–K'*). In the absence of Wnt or LiCl, HCQ had no effect on macropinocytosis (Fig. 2 *C* and *K*). In animal cap explants, *xWnt8* mRNA strongly stabilized microinjected CD63-RFP, reinforcing the view that the MVB compartment is expanded during Wnt signaling (*SI Appendix*, Fig. S2 *M–N'*).

We next tested whether expansion of the MVB/lysosome compartment with HCQ could increase dorsalization in vivo. Microinjection of LiCl (4 nL at 300 mM) into a single ventral blastomere of the four-cell *Xenopus* embryo resulted in slightly dorsalized embryos with enlarged head and cement gland structures (Fig. 3 *A* and *B*). Coinjection of HCQ and LiCl resulted in a remarkable potentiation of dorsal development, generating embryos consisting mostly of head structures with reduced or absent trunks (Fig. 3 *C*, *G*, and *H*). This dorsalizing effect of HCQ was specific to LiCl and was not seen in NaCl controls (*SI Appendix*, Fig. S4 *A–D*). The effects of HCQ occurred over a narrow concentration range in cultured cells, but, in the *Xenopus* embryo, dorsalizing effects were observed in the 1- to 10-mM range (in injections of 4 nL per embryo). At high HCQ levels (100 mM), no dorsalization was observed (*SI Appendix*, Fig. S4 *E–H*). We note that HCQ ventral injection of only 4 nL does not affect the endogenous dorsal axis, likely due to dilution. However, as will be seen below, interfering with lysosomal function with dorsal microinjections of EIPA or the V-ATPase V_0 subunit c inhibitors Baf and Concanamycin A inhibits axis formation.

EIPA is a Na^+/H^+ exchanger inhibitor derived from the diuretic amiloride that blocks macropinocytosis through alkalinization of the cortical cytoplasm, preventing actin polymerization (22, 23). Inhibition of the Na^+/H^+ exchanger may also affect endosomal acidification (23). No phenotypic effect was observed with single injections of HCQ or EIPA (Fig. 3 *D* and *E*), likely due to the dilution of only 4 nL introduced in the embryo. However, coinjection of 1 mM EIPA blocked the dorsalization phenotype caused by HCQ plus LiCl (compare Fig. 3*C* to Fig. 3*F*). Using *Krox20* as an in situ hybridization marker, the trunk shortening induced by LiCl and HCQ injection was reversed by coinjection of EIPA (Fig. 3 *I–L*; see brackets). The potentiation of dorsal development by HCQ and LiCl takes place early in development, for it greatly increased expression of the cytoplasmic determinant target genes *Siamois* and *Xnr3* at the blastula stage, as determined by qRT-PCR (Fig. 3*M*). EIPA inhibited the increased *Siamois and Xnr3* levels (Fig. 3*M*) as well as V-ATPase subunit V0a3 stabilization

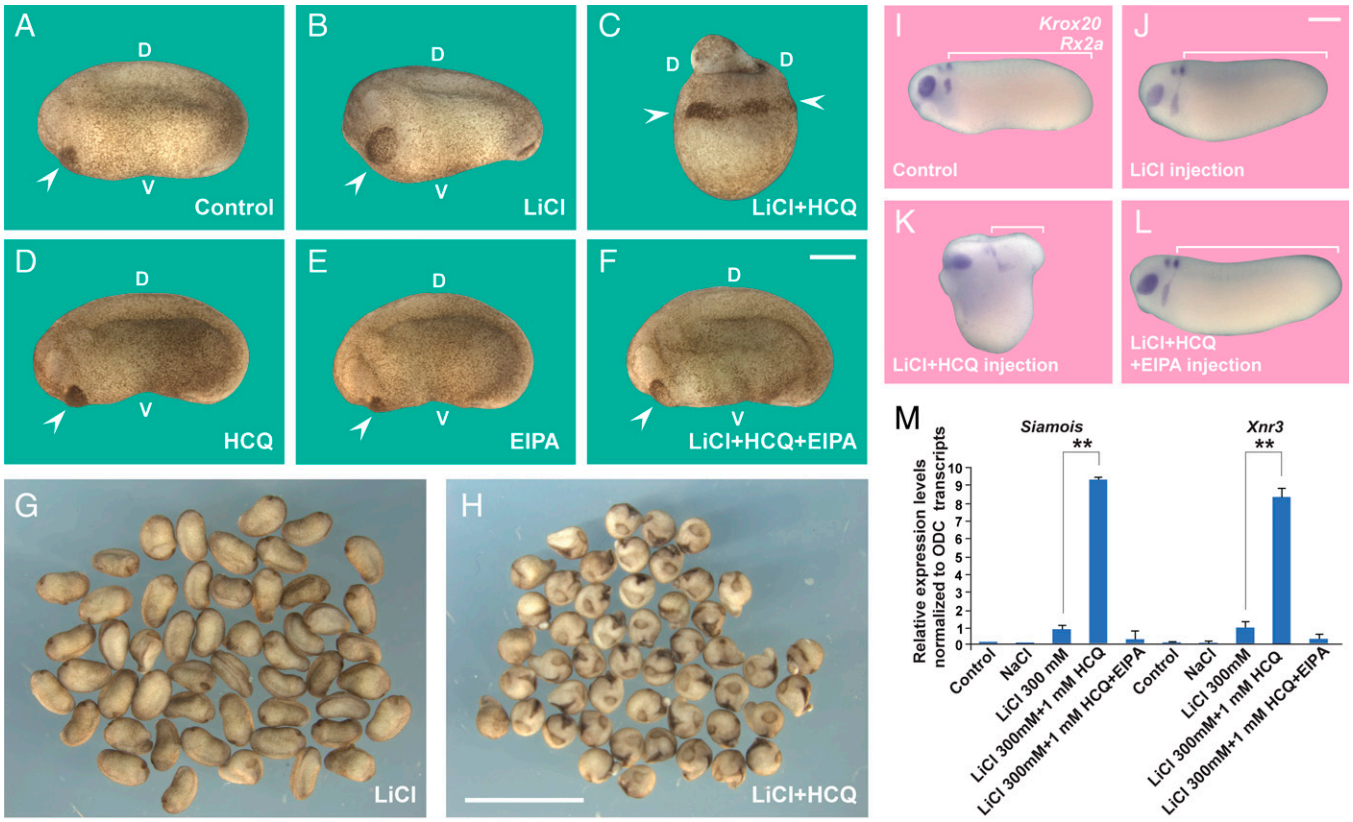

Fig. 3. Dorsalization by LiCl microinjection is potentiated by HCQ in *Xenopus*. Embryos were microinjected with 4 nL of 300 mM LiCl, 1 mM HCQ, 1 mM EIPA, or their combinations one time ventrally at the four-cell stage. (*A*) Uninjected control embryo at stage 24. (*B*) LiCl moderately dorsalizes the embryo. (*C*) Low-dose HCQ strongly cooperates with LiCl. (*D* and *E*) HCQ or EIPA alone are without phenotype. (*F*) The macropinocytosis inhibitor EIPA blocks the dorsalization caused by LiCl plus HCQ. (*G* and *H*) Panoramic comparison of LiCl alone and LiCl plus HCQ. (*I–L*) In situ hybridization with *Krox20* (hindbrain) and *Rx2a* (eye) markers showing that the trunk is reduced (brackets) and the head is expanded in embryos dorsalized by LiCl plus HCQ. Note rescue of trunk structures by EIPA. (*M*) The qRT-PCR at blastula stage 9.5 of the Wnt target genes Siamois and Xnr3 normalized for Ornithine decarboxylase (ODC). Note that low-concentration HCQ strongly enhances the response to microinjected LiCl, that this is blocked by EIPA, and that NaCl serves as a control for LiCl. Arrows indicate cement glant; D, dorsal; V, ventral. Numbers of embryos analyzed (five independent experiments) were as follows: A = 182; B = 137; C = 174; D = 142; E = 115. (Scale bars in *F* and *K*, 500 μm; scale bar in *H*, 5 mm.) Experiments in *I* represent biological triplicates; error bars denote SEM ($n \geq 3$) (**$P < 0.01$). See also *SI Appendix*, Fig. S4.

(*SI Appendix*, Fig. S1 *B* and *C*'). In addition, LiCl plus HCQ cooperated in stabilizing β-catenin protein on the dorsal side at blastula, and this was blocked by EIPA (*SI Appendix*, Fig. S4 *I–N*'). We conclude that low-dose HCQ increases activation of the Wnt signaling pathway at early stages of development and that this effect requires macropinocytosis.

Lysosomes Are Required for the Early Cytoplasmic Determinant Signal in *Xenopus*. We next tested whether lysosomes are required for activation of the dorsal early Wnt signal. The period of peak sensitivity of LiCl treatment has been carefully analyzed in *Xenopus* embryos and corresponds to the 32-cell stage (17). Our results indicated that dorsal lysosomes were already activated by LiCl at the 64-cell stage (Fig. 1). Therefore, we titrated brief treatments of whole embryos by immersion in the lysosomal inhibitor Baf at the 32-cell stage. Treatment with the V-ATPase inhibitor Baf at 5 μM for only 7 min before washing was found to be optimal. This brief treatment with Baf resulted in microcephalic embryos with no cement glands, in which the small head region was weakly pigmented while the ventroposterior epidermis contained most of the maternal pigment (Fig. 4 *A* and *B*). At the early tailbud stage, the CNS marker *Sox2* was inhibited, reflecting the microcephaly (Fig. 4 *C* and *D*).

Immersion in LiCl resulted in radial dorsal tadpole-stage embryos with increased panneural Sox2 expression surrounding the blastopore, while subsequent incubation with Baf at the 32-cell stage inhibited CNS induction (*SI Appendix*, Fig. S5 *A–C*'). The dominant effect of the lysosomal acidification inhibitor Baf agrees with the increased membrane trafficking and lysosomal acidification elicited by Wnt treatment of GSK3

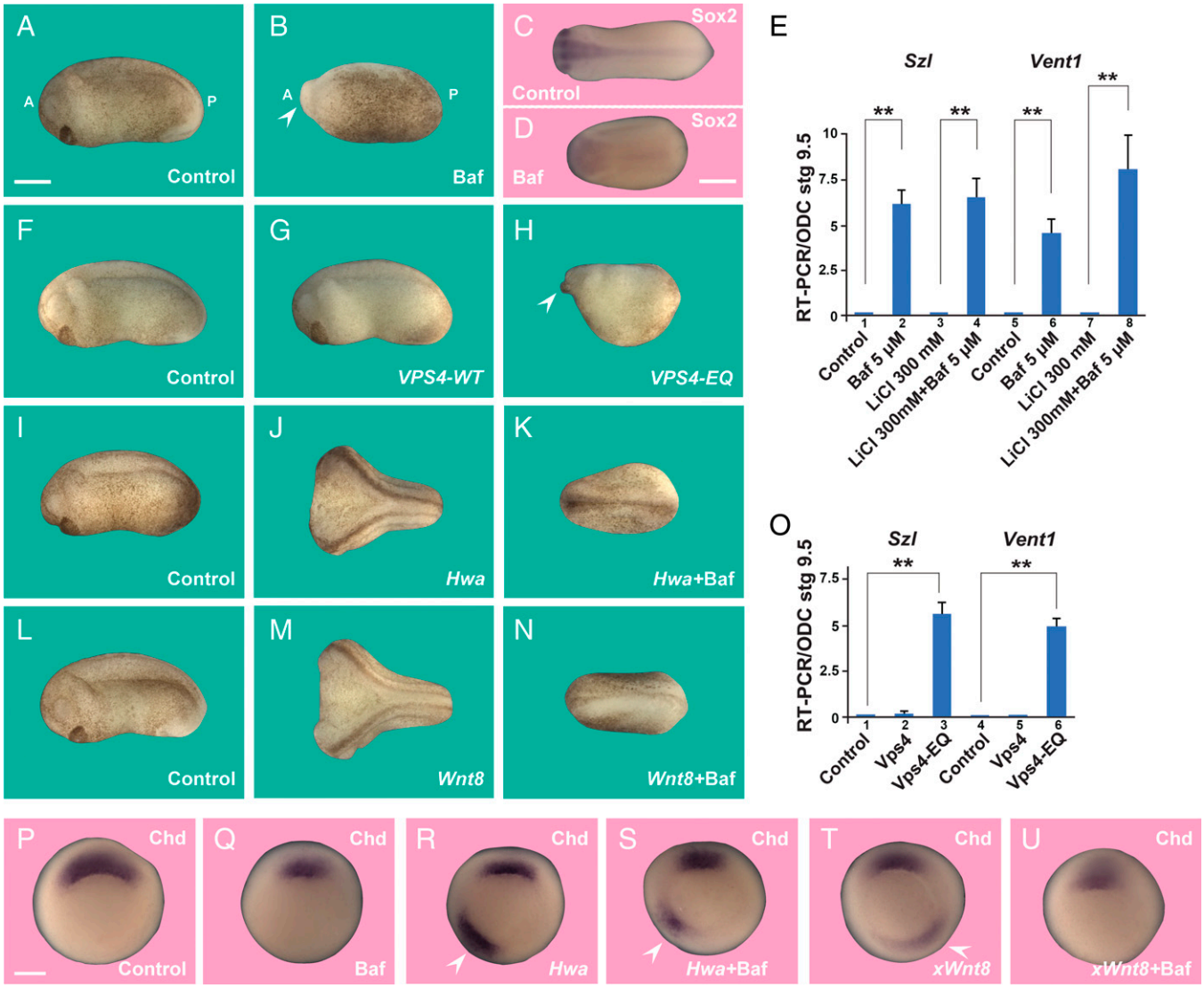

Fig. 4. Dorsal cytoplasmic determinant activity requires lysosomal acidification and the ESCRT machinery; Hwa signaling is inhibited by Bafilomycin. (*A* and *B*) Immersion of *Xenopus* embryos at the 32-cell stage in 5 μM Baf for 7 min results in a partially ventralized phenotype with microcephaly, loss of cement gland, and pigmentation in ventral and posterior ectoderm. A, anterior; P, posterior. (*C* and *D*) Baf reduces the panneural marker *Sox2*. (*E–G*) Inhibiting ESCRT machinery with Vps4-EQ, but not Vps4-WT, mRNA (two dorsal injections of 400 pg at the four-cell stage) reduces axis formation. Arrowhead indicates microcephaly. (*H–J*) Microinjection of *xHwa* mRNA (10 pg one time ventrally at the four-cell stage) induces complete secondary axes that are blocked by Baf incubation at the 32-cell stage. (*K–M*) The *xWnt8* mRNA second axes are also inhibited by the V-ATPase inhibitor Baf. (*N*) The qRT-PCR of blastula embryos showing that Baf treatment at the 32-cell stage increases expression of the ventral markers *Szl* and *Vent1* in wild-type and LiCl-treated embryos. (*O*) The qRT-PCR of blastula embryos showing that inhibiting the ESCRT machinery with the Vps4-EQ point mutation increases transcription of the ventral markers *Szl* and *Vent1* in *Xenopus*. (*P–U*) In situ hybridizations of *chordin* at the gastrula stage showing partial inhibition of the organizer by Baf in control, Hwa, and xWnt8 axes; arrowheads indicate ectopic *chd* expression. Numbers of embryos analyzed were as follows: A = 94; B = 77; E = 89; F = 62; G = 46; H = 235; I = 67; J = 71; K = 182; L = 57; M = 70 (two independent experiments). (Scale bars, 500 μm.) The qRT-PCR experiments represent biological triplicates; error bars denote SEM ($n \geq 3$) (**$P < 0.01$). See also *SI Appendix*, Figs. S5–S8.

inhibition in mammalian cultured cells reported previously (10). We tested other GSK3 inhibitors, BIO (6-bromoindirubin-3′-oxime) and CHIR99021, which could also be blocked by Bafilomycin A (*SI Appendix*, Fig. S6). In addition, inhibition of the endogenous dorsal axis could be obtained by microinjecting EIPA or the V-ATPase inhibitor Concanamycin A into two dorsal blastomeres at the four-cell stage (4 nL of 2 or 1 mM) (*SI Appendix*, Fig. S7 *A* and *B*′). Incubation of whole embryos at the 32-cell stage with Concanamycin A (5 μM for 7 min) also resulted in ventralization (*SI Appendix*, Fig. S7 *C* and *C*′). Dorsal microinjection of Baf caused ventralization (*SI Appendix*, Fig. S7 *D* and *D*′) similar to that caused by immersing embryos at the 32-cell stage (Fig. 2 *A* and *B*). We conclude that endogenous embryonic axis formation requires the function of early lysosomes.

Wnt signaling requires endocytosis and the sequestration of GSK3 in MVB/endolysosomes via the ESCRT machinery (9, 10). Vacuolar protein sorting 4 (Vps4) is an ATPase essential for the final steps of MVB intraluminal vesicle formation and has a very effective dominant-negative point mutation (Vps4-EQ) that blocks its function (24). Microinjection of Vps4-EQ mRNA into each dorsal blastomere at the four-cell stage reduced axial development and resulted in microcephalic embryos and, importantly, this inhibition was specific, since Vps4-WT had no discernable effect on the embryo (Fig. 4 *E*–*G*). Microinjection of the validated antisense reagent Hrs-MO (9) also inhibited anterior and dorsal development (*SI Appendix*, Fig. S8*A*). These results indicate that dorsal lysosomes and components of the MVB membrane trafficking machinery are required for the full activity of the endogenous dorsal signal in *Xenopus* embryos.

Hwa is a maternal mRNA encoding a novel transmembrane protein translated specifically in dorsal blastomeres in zebrafish and *Xenopus* embryos. It is likely that Hwa is a key component of the mysterious dorsal cytoplasmic determinant activated after fertilization (5). When microinjected into a ventral blastomere at the four- to eight-cell stage, *Hwa* mRNA induced complete secondary axes with high efficiency (Fig. 4 *H* and *I*). This result provides confirmation by an independent laboratory that *xHwa* mRNA has potent inductive effects (5). Since dorsal development required lysosomal acidification, we also tested whether Baf treatment inhibited Hwa function. We found that 7-min incubation of 32-cell embryos with the V-ATPase inhibitor Baf strongly inhibited secondary and primary axis formation in Hwa-injected embryos (Fig. 4 *H*–*J*). Coinjection of Hwa mRNA with EIPA or Hrs-MO blocked Hwa inductive activity, further strengthening the view that Hwa requires the membrane trafficking machinery (*SI Appendix*, Fig. S8 *B*–*E*). We also examined the effect of Baf in *xWnt8* mRNA–injected embryos, in which the same signaling pathway is activated. It was found that Baf blocked the Wnt8 twinning phenotype (Fig. 4 *K*–*M*).

Molecular analyses indicate that the ventralizing effects of Baf occur early in embryogenesis. When transcripts were analyzed at the blastula stage, the effect of the brief treatment with the lysosomal acidification inhibitor Baf induced a sharp increase of the ventral development marker genes *Sizzled* (*Szl*) and *Vent1* by qRT-PCR (Fig. 4*N*, lanes 2 and 6). In LiCl-immersed embryos (300 mM, 7-min incubation at 32 cells) (17), the ventral markers *Szl* and *Vent1* were also strongly induced by subsequent treatment with Baf (Fig. 4*N*, lanes 4 and 8). The ventralizing effects of interfering with MVB formation occur early in development for VPS4-EQ, but not Vps4-wt, resulted in a significant increase of *Sizzled* and *Vent1* transcripts before the onset of gastrulation (Fig. 4*O*). In addition, Baf treatment partially inhibited expression of the Spemann organizer molecular marker Chordin (Chd) in endogenous, Hwa, and xWnt8 axes (Fig. 4 *P*–*U*). Taken together, the results indicate that lysosome activity and MVB formation are required for Wnt signaling starting at the 32-cell stage.

Discussion

The main conclusion of the present study is that lysosomes play an essential role in the establishment of the initial polarity of the body axis in *Xenopus* embryos. As indicated in the diagram in Fig. 5, recent work has implicated membrane trafficking as a key step in the activation of Wnt signaling (10). After fertilization, a microtubule-driven cortical rotation of the egg generates the first asymmetry in the egg, resulting in a dorsal Wnt-like signal (Fig. 1*A*′) (3, 4). Wnt signaling causes a remarkable increase in macropinocytosis, as well as lysosomal activation and acidification, even in the absence of new protein synthesis (12, 13). As the role of lysosomes in development was largely unexplored, we examined the localization of active lysosomes at the 64-cell stage, just after the period of peak sensitivity to GSK3 inhibition by LiCl (17). Lysosomes containing activated cathepsin D were enriched in dorsal marginal cells, particularly in embryos microinjected with Wnt or LiCl (Fig. 1). Involvement of the MVB/lysosome compartment was suggested by the marked increase in dorsalization by LiCl at low doses, but not high doses, of HCQ that expanded the MVB compartment marked by CD63. The transit through intraluminal vesicles of MVBs is a required step for the trafficking of plasma membrane proteins into lysosomes (10). A pulse of the lysosome acidification inhibitor Baf at the 32-cell stage increased ventral markers and decreased endogenous Spemann organizer formation, as did interfering with the ESCRT machinery that forms MVBs.

The early Wnt signal may modify the response of the embryo to other growth factor signaling pathways. For example, it is known that Wnt-induced inhibition of Smad4 phosphorylation by GSK3 increases the intensity and duration of TGF-β/Nodal signaling (25). The activity of the Smad4 transcription factor, which functions in both the Activin/TGF-β and BMP pathways, is also increased by FGF/MAPK phosphorylations (25). In addition, it is known that receptor tyrosine kinases transiently activate macropinocytosis (10, 23). Thus, there is considerable potential for cross-regulation of the early lysosomal signal with other pathways, which will be investigated in the future.

In mammalian cells, low-dose HCQ increased Wnt signaling, but only within narrow ranges of concentration. It is conceivable that some of the clinical prophylactic antimalarial and antiautoimmune effects of HCQ might be mediated by increased macropinocytosis and lysosomal activity in small populations of Wnt-activated immune cells, rather than lysosomal inhibition as is currently thought (26, 27).

The recent discovery of the maternal Hwa transmembrane protein has suggested that, after fertilization in dorsal cells, Hwa, rather than a canonical Wnt–Lrp6 interaction, is responsible for the dorsal maternal signal (5, 28). Hwa is a plasma membrane protein with a short extracellular domain and a large intracellular domain that functions by promoting the degradation of Axin1 in zebrafish and *Xenopus* embryos (5). In a mammalian cell system, zebrafish Hwa binds to Axin1 and promotes its degradation with the involvement of tankyrases (5). The tumor suppressor Axin1, which is a GSK3-binding protein, is a component of the β-catenin destruction complex, and its

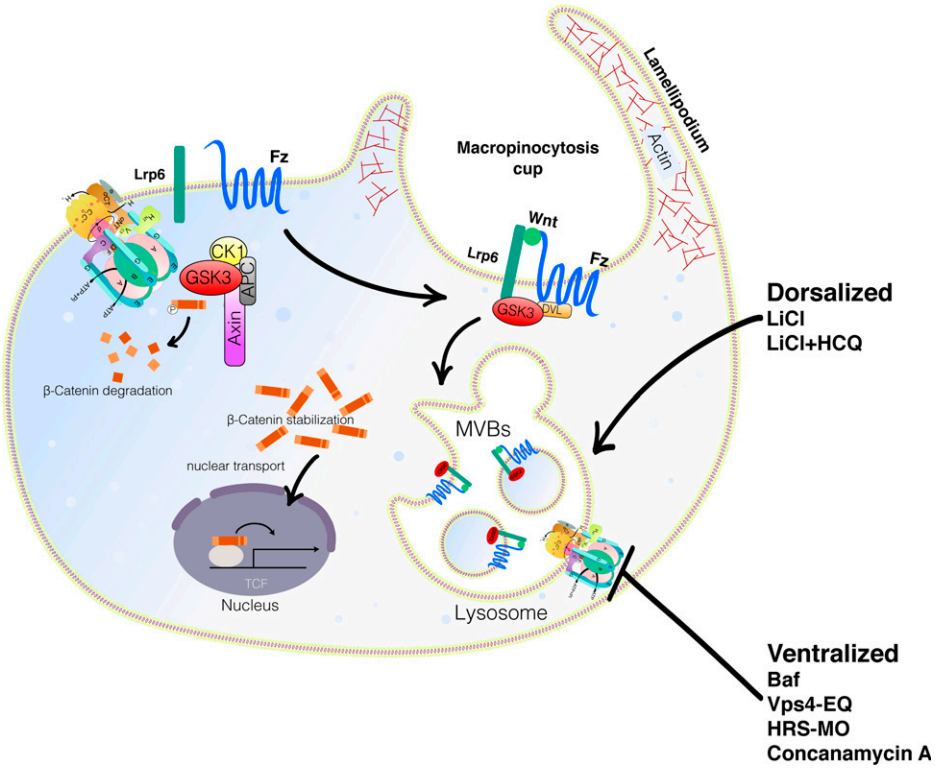

Fig. 5. Model of membrane trafficking during Wnt signaling highlighting the role of macropinocytosis, V-ATPase, MVBs, and lysosomes. Binding of Wnt to the Frizzled (Fz) and Lrp6 receptors results in a local inhibition of GSK3 activity that induces the actin machinery to form lamellipodia that engulf large amounts of liquid through macropinocytosis. In the presence of Wnt, plasma membrane is trafficked into MVBs that become lysosomes as they are activated by progressively decreasing pH. V-ATPase pumps protons into the lysosomal lumen, driving lysosomal acidification. Inhibiting V-ATPase (Baf or Concanamycin A) or MVB formation (Vps4-EQ or Hrs-MO) results in microcephalic embryos with increased ventral structures. LiCl mimics Wnt signaling by inhibiting GSK3, and low-dose HCQ expands the MVB compartment, facilitating Wnt signaling in mammalian cells and the dorsalization of *Xenopus* embryos.

degradation stabilizes β-catenin, leading to the transcriptional activation of the Wnt signaling pathway (6, 28).

Importantly, a recent report from the Tao laboratory showed that Hwa protein in blastomeres outside the presumptive dorsal progenitors is ubiquitinated by the transmembrane E3 ubiquitin ligase zinc and ring finger 3 (ZNRF3), and then subjected to degradation through the lysosomal pathway (29). This mechanism serves to limit or dampen Spemann organizer formation in the ventral side of the embryo (29). Our results suggest that Hwa proteins in presumptive dorsal progenitors might be macropinocytosed into MVBs, and therefore protected from proteasomal degradation, and remain active in mediating dorsal development. Work from our laboratory indicates that the lysosomal membrane trafficking pathway is a required step in the canonical Wnt signaling pathway (12, 13). We propose that, on the dorsal side of the early embryo, nonubiquitinated Hwa may bind Axin1 and is trafficked into lysosomes together with GSK3, resulting in the sequestration of GSK3 to generate a Wnt-like signal. In the future, it will be interesting to investigate whether endogenous Hwa protein colocalizes with GSK3 in dorsal MVBs/lysosomes in early *Xenopus* embryos.

In addition to Hwa and lysosomes, other mechanisms function in the control of activation of β-catenin signaling and dorsal organizer formation. Putative cytoplasmic membrane organelles containing Dvl are translocated from the vegetal pole to the dorsal marginal zone (3, 4). Further, maternal GSK3 Binding Protein (GBP/Frat) is required for dorsal development, inhibiting GSK3 function by preventing Axin1 from binding GSK3 (30, 31), as are microtubules, kinesin motors, and the adaptor protein Syntabulin that bridges the binding of kinesin to vesicular membrane proteins (32, 33). Much remains to be learned about the activation of the embryonic early Wnt pathway in *Xenopus* embryos.

How does Wnt signaling regulate lysosome activation? Previous work has shown that the activated Wnt Lrp6 receptor binds to the peripheral V-ATPase protein ATP6AP2 (also called Prorenin receptor) (8). ATP6AP2 binds to transmembrane protein 9 (TMEM9), which, in turn, binds to and activates the V-ATPase that acidifies lysosomes (34). TMEM9 is an MVB protein that induces secondary axes in *Xenopus* embryos and plays an oncogenic role in colorectal (CRC) and hepatocellular (HCC) carcinomas (35). Treatment with Baf reduces tumor growth in TMEM9-expressing CRC and HCC xenografts, indicating an important role for lysosomes in tumor progression (34). It is possible that, in the *Xenopus* embryo, V-ATPase and lysosomal trafficking is activated on the dorsal side by a similar TMEM9–V-ATPase activation. A way to investigate further the molecular mechanism would be to isolate lysosome or MVBs fractions from embryos and then inject these fractions ventrally to see whether they create a secondary axis, but this is difficult in yolky eggs such as *Xenopus*. In sum, the results presented here indicate that membrane trafficking, macropinocytosis, V-ATPase, and lysosomes are essential for the earliest developmental decisions in the *Xenopus* vertebrate development model system.

Materials and Methods

Reagents and Antibodies. SiR-Lysosome was purchased from Cytoskeleton (CYSC012, used at 1 μM).

HCQ (H0915), CQ diphosphate (C 6628), EIPA (A3085), LiCl and sodium chloride (NaCl) (S9888), IPA-3 (I2285, used at 2.5 μM), and Concanamycin A

(C9705, used at 5 μM) were obtained from Sigma. Baf (S1413) was purchased from Selleckchem. TMR-dextran 70,000 kDa was purchased from ThermoFisher (D1818). Total β-catenin antibody (1:1,000) was purchased from Invitrogen (712700), glyceraldehyde-3-phosphate dehydrogenase antibody (1:1,000) was obtained from cell signaling, anti-ATP6V0a3 antibody (23) was obtained from Novus (nbp1-89333, 1:1,000). Antibodies against Pak1 (ab131522) and Ras (ab52939) and secondary antibodies for immunostaining (ab150083, ab150117) (1:500) were obtained from Abcam. Wnt3a protein was from Peprotech (315-20) and used at 100 ng/mL. Hrs-MO TGCCGCTTCCTCTTCCCATTGCGAA (9) was from Gene Tools and microinjected as 4 nL of 0.3 mM MO.

Tissue Culture. HEK-293BR (BAR/Renilla) were cultured in Dulbecco's modified Eagle's medium (DMEM) containing 10% fetal bovine serum (FBS); SW480 cells and SW480APC cells (36) were cultured at 37 °C in 5% CO_2 atmosphere in DMEM/F12 (DMEM: Nutrient Mixture F-12), supplemented with 5% FBS, 1% glutamine, and penicillin/streptomycin. The cells were seeded at a cell density of 20 to 30%, and experiments were performed when cells reached a confluence of 70 to 80%. Cells were cultured 6 h to 8 h in medium containing 2% FBS before treatments.

***Xenopus* Embryo Microinjection and In Situ Hybridization.** *Xenopus laevis* embryos were fertilized in vitro using excised testes and cultured and staged as described (33). Ventral coinjection of 4 nL of LiCl (300 mM) ± HCQ (1 mM to 2 mM) was performed at the two- to four-cell stage and cultured until the early tadpole stage. EIPA was injected at 1 mM. The pCS2+ clones encoding *xWnt8*, x*Hwa*, CD63-RFP, mGFP, Vps4-wt, and Vps4-EQ were linearized with NotI and transcribed with SP6 RNA polymerase using the Ambion mMessage mMachine kit (9). Embryos were injected in 1× MMR (Marc's modified Ringers) saline and cultured in 0.1× MMR. In vitro synthesized mRNAs were microinjected in a 4-nL volume using an IM 300 Microinjector (Narishige International USA, Inc.). To study the role of ESCRT in development, *Xenopus* antisense HRS-MO (9) was injected two times dorsally at the four-cell stage. In situ hybridizations were performed as described previously at http://www.hhmi.ucla.edu/derobertis.

Bisected Embryo Lysosome Staining. Embryos at the two- to four-cell stage were injected once into a vegetal blastomere with LiCl (300 mM) or *xWnt8* (2 pg). Embryos were incubated in 0.1× MMR solution until the 64-cell stage or stage 9. Embryos were collected and fixed with 4% PFA (paraformaldehyde, Thermo Scientific, 28908) diluted in 1× PBS (Fisher Scientific, BP399-4). After 24 h of fixation, embryos were cut along the D–V axis with a surgical blade and refixed with 4% PFA for 15 min. Embryos were then washed with PBS three times, blocked with 5% bovine serum albumin (BSA) in PBS to reduce the background for 24 h, and incubated with 1 μM Sir-Lysosome marker for active lysosomal marker cathepsin D for 2 h, then washed three times with PBS. Samples were imaged using an Axio Zoom.V16 Stereo Zoom Zeiss microscope with Apotome function, and stacked images were reconstructed using the Zen 2.3 Pro Zeiss software. For embryo stainings with V-ATPase subunit V0a3 or β-catenin antibodies, after the BSA blocking treatment, samples were incubated with the primary antibody (1:300) overnight, washed, and incubated with the secondary antibody also overnight (1:500). Embryos were plated in agar Petri dishes with PBS for microscopic examination as soon as possible to avoid the loss of fluorescence.

Animal Cap Cell Culture. Animal caps were dissected at early blastula stage 8.5 to 9 in 1× MMR solution and washed three times, and cells were cultured in L-15 medium containing 10% fetal calf serum diluted to 50% with H_20 (37) on fibronectin-coated 35-mm Petri dishes with glass bottoms (#0 cover glass, Cell E&G: GBD00003-200) for 12 h to 18 h. When mounting with coverslips, a drop of Anti-fade Fluorescence Mounting Medium-Aqueous, Fluoroshield (ab104135) was added, and microscopic examination of RFP and GFP was performed. Image acquisition was performed using a Carl Zeiss Axio Observer Z1 Inverted Microscope with Apotome.

Immunostainings of Mammalian Cells. HEK293T and SW480 ± APC cells were plated on glass coverslips. Coverslips were acid washed and treated with 10 μg/mL fibronectin (Sigma F4759) for 30 min at 37 °C to enhance cell spreading and adhesion. Cells were fixed with 4% PFA (Sigma #P6148) in PBS for 15 min, permeabilized with 0.2% Triton X-100 in PBS for 10 min, and blocked with 5% BSA in PBS for 1 h. Primary antibodies (1:100) were added overnight at 4 °C. The samples were washed three times with PBS, and secondary antibodies were applied for 1 h at room temperature (1:1,000). After three additional washes with PBS, coverslips were mounted with Fluoroshield Mounting Medium with DAPI (ab104139). Immunofluorescence was analyzed and photographed using a Zeiss Imager Z.1 microscope with Apotome.

TMR-Dextran Assay. HEK293T cells were plated on glass coverslips for 12 h to 18 h. Cells were then incubated at 37 °C in 5% CO_2 atmosphere with DMEM supplemented with 2% FBS, and 1 mg/mL TMR for 1 h. After incubation, cells were washed, fixed, and blocked for 1 h with 5% BSA in PBS to reduce background from nonspecific binding. The coverslips were mounted with Fluoroshield Mounting Medium with DAPI (ab104139). Immunofluorescence was analyzed and photographed using a Zeiss Imager Z.1 microscope with Apotome and using the Zen 2.3 imaging software.

Western Blots and Luciferase Assays. Cell lysates were prepared using RIPA buffer (0.1% Nonidet P-40, 20 mM Tris/HCl pH 7.5), 10% glycerol, together with protease (Roche #04693132001) and phosphatase inhibitors (Calbiochem #524629) and processed as described (12). Stable cell line HEK-293-BR expressing firefly and Renilla luciferase genes (12) was incubated for 12 h to 18 h with Wnt3a (100 ng/mL) or LiCl (40 mM) plus or minus HCQ (15 μM to 90 μM) or with HCQ alone. Luciferase activity was measured with the Dual-Luciferase Reporter Assay System (Promega) according to the manufacturer instructions, using a Glomax Luminometer (Promega).

Measurement of TMR Uptake by Spectrophotometry. Cells were seeded to maintain a cell density between 20% and 30%, and experiments were performed when cells reached a confluence of 70 to 80%. Cells were starved with 2% BSA for 6 h to 12 h, then stimulated with Wnt3a (100 ng/mL) plus or minus HCQ (15 μM to 100 μM) for 12 h to 18 h in 96-well plates. After incubation, TMR-dextran 70 kDa was added to the medium for 1 h (1 mg/mL). Cells were washed three times with PBS, trypsinized, and transferred into a 96-well microplate for reading. The TMR-dextran 70 kDa (excitation/emission 555/580 nm) absorbance was quantified with a SpectraMax microplate reader using the Softmax pro 5.4.4 software. The conditions used for excitation/emission were 544/590 nm. Three independent measurements were performed for each sample in this quantitative assay.

Bafilomycin Treatments. Frog embryos at the 32-cell stage were incubated with Baf (5 μM) for 7 min in 0.1 MMR solution. After incubation, embryos were washed two times with 0.1 MMR solution and cultured overnight until the early tailbud tadpole stage. Embryos injected once ventrally at the four-cell stage with *xWnt8* (2 pg) or *Hwa* (10 pg) mRNA were incubated in 0.1× MMR solution until the 32-cell stage. Embryos were then transferred in 0.1× MMR solution containing Baf (5 μM) and incubated for 7 min. After that, the embryos were washed two times with 0.1× MMR solution and cultured until the tadpole stage.

EIPA and Baf Injections. Frog embryos at the four-cell stage were injected into two dorsal blastomeres with EIPA (4 nL at 2 mM) or Baf (1 mM in 20% L-15 culture medium) and cultured until the tadpole stage to generate microcephalic embryos.

LiCl and Concanamycin A Incubation. Whole embryos at the 32-cell stage were incubated with LiCl (300 mM) or Concanamycin A (5 μM in 20% L-15 culture medium) for 7 min. After that, embryos were quickly washed two times with 0.1× MMR solution and subsequently incubated for 7 min in 0.1× MMR solution containing 5 μM Baf. After the treatment, the embryos were washed two times with 0.1 MMR solution and cultured until the tadpole stage.

BIO Incubation. Frog embryos were incubated at the 32-cell stage with the GSK3 inhibitor BIO (30 mM) in the presence or absence of Baf (5 mM in 20% L-15 culture medium). At stage 9.5, embryos were washed two times with 0.1× MMR solution and cultured until the tadpole stage.

CHIR99021 Incubation. *Xenopus* embryos were incubated at the 32-cell stage with the GSK3 inhibitor CHIR99021 (60 μM) in the presence or absence of Baf (5 mM in 20% L-15 culture medium); embryos were cultured with the reagent until the tadpole stage. A long incubation time is required to obtain a dorsalized phenotype with CHIR99021.

Table 1. Primer sequences for qRT-PCR

Gene	Forward	Reverse
ODC	CAGCTAGCTGTGGTGTGG	CAACATGGAAACTCACACC
Siamois	AAGATAACTGGCATTCCTGAGC	GGTAGGGCTGTGTATTTGAAGG
Xnr3	CGAGTGCAAGAAGGTGGACA	ATCTTCATGGGGACACAGGA
Sizzled	GTCTTCCTGCTCCTCTGC	AACAGGGAGCACAGGAAG
Vent1	GGCACCTGAACGGAAGAA	GATTTTGGAACCAGGTTTTGAC

qRT-PCR. The qRT-PCR experiments using *Xenopus* embryos were performed as previously described (33). Primer sequences for qRT-PCR are given in Table 1.

Statistical Analyses. Data were expressed as means and SEMs. Statistical analysis of the data was performed using the Student *t* test; a *P* value of <0.01** was considered statistically significant for differences between means.

Data Availability. All study results are included in the article and/or *SI Appendix*.

ACKNOWLEDGMENTS. We are grateful to J. Monka, P. Sheladiya, and D. Geissert for technical assistance; Q. Tao for the xHwa expression construct; R. Moon for BAR reporters and xWnt8; M. Faux for SW480APC cells; Y. Moriyama, Y. Ding, P. Sheladiya, and J. Monka for comments on the manuscript; and M. F. Domowicz for help with the illustrations. This work was supported by the University of California Cancer Research Coordinating Committee (Grant C21CR2039); NIH Grant P20CA016042 to the University of California, Los Angeles Jonsson Comprehensive Cancer Center; and the Norman Sprague Endowment for Molecular Oncology.

1. J. Heasman, Patterning the early *Xenopus* embryo. *Development* **133**, 1205–1217 (2006).
2. S. Schneider, H. Steinbeisser, R. M. Warga, P. Hausen, Beta-catenin translocation into nuclei demarcates the dorsalizing centers in frog and fish embryos. *Mech. Dev.* **57**, 191–198 (1996).
3. B. A. Rowning *et al.*, Microtubule-mediated transport of organelles and localization of β-catenin to the future dorsal side of *Xenopus* eggs. *Proc. Natl. Acad. Sci. U.S.A.* **94**, 1224–1229 (1997).
4. C. A. Larabell *et al.*, Establishment of the dorso-ventral axis in *Xenopus* embryos is presaged by early asymmetries in β-catenin that are modulated by the Wnt signaling pathway. *J. Cell Biol.* **136**, 1123–1136 (1997).
5. L. Yan *et al.*, Maternal Huluwa dictates the embryonic body axis through β-catenin in vertebrates. *Science* **362**, eaat1045 (2018).
6. H. Clevers, R. Nusse, Wnt/β-catenin signaling and disease. *Cell* **149**, 1192–1205 (2012).
7. C. Niehrs, The complex world of WNT receptor signalling. *Nat. Rev. Mol. Cell Biol.* **13**, 767–779 (2012).
8. C. M. Cruciat *et al.*, Requirement of prorenin receptor and vacuolar H+-ATPase-mediated acidification for Wnt signaling. *Science* **327**, 459–463 (2010).
9. V. F. Taelman *et al.*, Wnt signaling requires sequestration of glycogen synthase kinase 3 inside multivesicular endosomes. *Cell* **143**, 1136–1148 (2010).
10. L. V. Albrecht, N. Tejeda-Muñoz, E. M. De Robertis, Cell biology of canonical Wnt signaling. *Annu. Rev. Cell Dev. Biol.* **37**, 369–389 (2021).
11. G. Redelman-Sidi *et al.*, The canonical Wnt pathway drives macropinocytosis in cancer. *Cancer Res.* **78**, 4658–4670 (2018).
12. N. Tejeda-Muñoz, L. V. Albrecht, M. H. Bui, E. M. De Robertis, Wnt canonical pathway activates macropinocytosis and lysosomal degradation of extracellular proteins. *Proc. Natl. Acad. Sci. U.S.A.* **116**, 10402–10411 (2019).
13. L. V. Albrecht *et al.*, GSK3 inhibits macropinocytosis and lysosomal activity through the Wnt destruction complex machinery. *Cell Rep.* **32**, 107973 (2020).
14. E. M. De Robertis, J. B. Gurdon, A brief history of *Xenopus* in biology. *Cold Spring Harb. Protoc.* **2021**, top107615 (2021).
15. J. Marciniszyn Jr., J. A. Hartsuck, J. Tang, Mode of inhibition of acid proteases by pepstatin. *J. Biol. Chem.* **251**, 7088–7094 (1976).
16. J. L. Christian, R. T. Moon, Interactions between Xwnt-8 and Spemann organizer signaling pathways generate dorsoventral pattern in the embryonic mesoderm of *Xenopus*. *Genes Dev.* **7**, 13–28 (1993).
17. K. R. Kao, Y. Masui, R. P. Elinson, Lithium-induced respecification of pattern in *Xenopus laevis* embryos. *Nature* **322**, 371–373 (1986).
18. C. Ramirez, A. D. Hauser, E. A. Vucic, D. Bar-Sagi, Plasma membrane V-ATPase controls oncogenic RAS-induced macropinocytosis. *Nature* **576**, 477–481 (2019).
19. R. Dobrowolski *et al.*, Presenilin deficiency or lysosomal inhibition enhances Wnt signaling through relocalization of GSK3 to the late-endosomal compartment. *Cell Rep.* **2**, 1316–1328 (2012).
20. T. L. Biechele, R. T. Moon, Assaying beta-catenin/TCF transcription with beta-catenin/TCF transcription-based reporter constructs. *Methods Mol. Biol.* **468**, 99–110 (2008).
21. J.-M. Escola *et al.*, Selective enrichment of tetraspan proteins on the internal vesicles of multivesicular endosomes and on exosomes secreted by human B-lymphocytes. *J. Biol. Chem.* **273**, 20121–20127 (1998).
22. M. Koivusalo *et al.*, Amiloride inhibits macropinocytosis by lowering submembranous pH and preventing Rac1 and Cdc42 signaling. *J. Cell Biol.* **188**, 547–563 (2010).
23. C. Commisso, R. J. Flinn, D. Bar-Sagi, Determining the macropinocytic index of cells through a quantitative image-based assay. *Nat. Protoc.* **9**, 182–192 (2014).
24. N. Bishop, P. Woodman, ATPase-defective mammalian VPS4 localizes to aberrant endosomes and impairs cholesterol trafficking. *Mol. Biol. Cell* **11**, 227–239 (2000).
25. H. Demagny, T. Araki, E. M. De Robertis, The tumor suppressor Smad4/DPC4 is regulated by phosphorylations that integrate FGF, Wnt, and TGF-β signaling. *Cell Rep.* **9**, 688–700 (2014).
26. I. Ben-Zvi, S. Kivity, P. Langevitz, Y. Shoenfeld, Hydroxychloroquine: From malaria to autoimmunity. *Clin. Rev. Allergy Immunol.* **42**, 145–153 (2012).
27. Z. N. Lei *et al.*, Chloroquine and hydroxychloroquine in the treatment of malaria and repurposing in treating COVID-19. *Pharmacol. Ther.* **216**, 107672 (2020).
28. C. Niehrs, The role of *Xenopus* developmental biology in unraveling Wnt signalling and antero-posterior axis formation. *Dev. Biol.* **482**, 1–6 (2022).
29. X. Zhu *et al.*, Lysosomal degradation of the maternal dorsal determinant Hwa safeguards dorsal body axis formation. *EMBO Rep.*, **22**, e53185 (2021).
30. C. Yost *et al.*, GBP, an inhibitor of GSK-3, is implicated in *Xenopus* development and oncogenesis. *Cell* **93**, 1031–1041 (1998).
31. G. H. Farr 3rd *et al.*, Interaction among GSK-3, GBP, axin, and APC in *Xenopus* axis specification. *J. Cell Biol.* **148**, 691–702 (2000).
32. C. Weaver *et al.*, GBP binds kinesin light chain and translocates during cortical rotation in *Xenopus* eggs. *Development* **130**, 5425–5436 (2003).
33. G. Colozza, E. M. De Robertis, Maternal *syntabulin* is required for dorsal axis formation and is a germ plasm component in *Xenopus*. *Differentiation* **88**, 17–26 (2014).
34. Y. S. Jung *et al.*, TMEM9 promotes intestinal tumorigenesis through vacuolar-ATPase-activated Wnt/β-catenin signalling. *Nat. Cell Biol.* **20**, 1421–1433 (2018).
35. Y. S. Jung *et al.*, TMEM9-v-ATPase activates Wnt/β-Catenin signaling via APC lysosomal degradation for liver regeneration and tumorigenesis. *Hepatology* **73**, 776–794 (2021).
36. M. C. Faux *et al.*, Restoration of full-length adenomatous polyposis coli (APC) protein in a colon cancer cell line enhances cell adhesion. *J. Cell Sci.* **117**, 427–439 (2004).
37. J. C. Smith, J. R. Tata, Xenopus cell lines. *Methods Cell Biol.* **36**, 635–654 (1991).